Chimica et Natura Acta
p-ISSN: 2355-0864 e-ISSN: 2541-2574
Homepage: http://jurnal.unpad.ac.id/jcena

The Role of Glu/Gly/Zif-8 Edible Film in Improving the Superior Rheological and Water Vapor Barrier Properties and Antibacterial Activity for Active Food Packaging

Nancy Siti Djenar, Kardian Rinaldi*, Dina Nur Rahma, Dina Kustiana
Department of Chemical Engineering, Politeknik Negeri Bandung, Jl. Gegerkalong Hilir, Ciwaruga, Kec. Parongpong, Kabupaten Bandung Barat, Jawa Barat, 40012
*Corresponding author: kardian.rinaldi@polban.ac.id

DOI: https://doi.org/10.24198/cna.v14.n1.66715
Article history: Received 17 September 2025 | Revised 22 November 2025 | Accepted 31 December 2025

Abstract: The low barrier to water vapor and gas is a critical limitation of glycerol-plasticized gluten-based edible films (GBEF) for food packaging applications. In this study, gluten (Glu) and glycerol (Gly) were cross-linked with 0.25–1.00% (w/v) zeolitic imidazolate framework-8 (ZIF-8) to improve interfacial compatibility and enhance the structural integrity of the film matrix. The formation of hydrogen bonds and electrostatic interactions between ZIF-8 and the Glu/Gly matrix strengthened the chemical network, resulting in increased tensile strength (TS). The water vapor transmission rate (WVTR) of Glu/Gly/ZIF-8 edible films (Glu/Gly/ZIF-8 EF) ranged from 1.085 to 1.453 g/m²/24 h, indicating significantly improved barrier properties. Mechanical testing showed TS and elongation at break (EAB) values of 32.18–60.58 MPa and 211.86–382.83%, respectively, meeting Japanese Industrial Standards for edible films (TS > 0.3 MPa, EAB > 70%, WVTR < 10 g/m²/24 h, thickness < 0.25 mm). Glu/Gly/ZIF-8 EF also demonstrated strong antibacterial activity, with inhibition zones of 25–26 mm for Gram-negative Escherichia coli and 25–34 mm for Gram-positive Staphylococcus aureus. These findings demonstrate that ZIF-8 effectively enhances both the mechanical and functional performance of gluten/glycerol films, providing a promising strategy to expand their application as bioactive packaging materials in the food industry.

Keywords: antibacterial, gluten, Glu/Gly/ZIF-8 EF, glycerol, ZIF-8

Abstrak: *Rendahnya kemampuan penghalang uap air dan gas merupakan keterbatasan utama pada film edible berbasis gluten yang diplastisisasi gliserol (GBEF) untuk aplikasi pengemasan pangan. Penelitian ini mengkaji pengaruh penambahan 0,25–1,00% (b/v) kerangka imidazolat zeolitik-8 (ZIF-8) terhadap kompatibilitas antarmuka, integritas struktural, serta sifat fungsional matriks film Glu/Gly. Pembentukan ikatan hidrogen dan interaksi elektrostatik antara ZIF-8 dan matriks Glu/Gly memperkuat jaringan kimia, sehingga meningkatkan kekuatan tarik (TS). Hasil pengukuran menunjukkan bahwa laju transmisi uap air (WVTR) film Glu/Gly/ZIF-8 berkisar antara 1,085–1,453 g/m²/24 jam, menandakan peningkatan sifat penghalang secara signifikan. Sementara itu, TS dan elongasi putus (EAB) masing-masing berada pada rentang 32,18–60,58 MPa dan 211,86–382,83%, memenuhi persyaratan Standar Industri Jepang (TS > 0,3 MPa; EAB > 70%; WVTR < 10 g/m²/24 jam; ketebalan < 0,25 mm). Film ini juga menunjukkan aktivitas antibakteri terhadap Escherichia coli (zona hambat 25–26 mm) dan Staphylococcus aureus (zona hambat 25–34 mm). Hasil penelitian ini menunjukkan bahwa ZIF-8 secara efektif meningkatkan kinerja mekanis dan fungsional film Glu/Gly, sehingga memiliki potensi sebagai bahan kemasan bioaktif untuk industri pangan.*

Kata kunci: *antibakteri, gluten, Glu/Gly/ZIF-8 EF, gliserol, ZIF-8*

INTRODUCTION

The technological development of edible films as food packaging materials has primarily focused on the incorporation of components that improve nutritional value while avoiding adverse effects. (Kumar *et al.* 2022; Pires *et al.* 2024). Edible films, derived from natural biomacromolecules such as polysaccharides, proteins, and lipids, represent an alternative approach to conventional food packaging. Among plant-based proteins, wheat gluten is a promising material for edible film formation. It is composed primarily of two protein fractions, gliadin and glutenin, both of which contribute to the distinctive structural and functional properties of gluten (Xu & Li 2023; Zhang *et al.* 2020; Barazi *et al.* 2023; Djenar *et al.* 2024a). Wheat gluten is further valued for its edibility, biodegradability, wide availability, low cost, excellent gas barrier properties,

and good mechanical strength, the latter of which arises from the presence of intra- and intermolecular disulfide bonds (Xu & Li 2023; Zhang *et al.* 2020; Djenar *et al.* 2024b; Abdullah-Al-Rahim 2021). Gluten-based edible films (GBEFs) plasticized with 3.5% glycerol and 1.0% olive oil exhibit antimicrobial activity, complying with the requirements of the Japanese Industrial Standards (JIS) (Wang *et al.* 2022).

Despite significant progress in enhancing the physicochemical and antimicrobial performance of gluten-based edible films (GBEFs) through the incorporation of inorganic nanoparticles (e.g., ZnO) (Sharanyakanth & Radhakrishnan 2020; Djenar *et al.* 2024b; Khashayary & Aarabi 2021), these systems still face important limitations. For instance, studies have shown that while ZnO nanoparticles can reduce water vapor transmission rate (WVTR), improve gas-barrier properties, and enhance tensile strength and elongation at break, concerns regarding nanoparticle agglomeration, control over ion release, potential migration into food, and long-term environmental/health effects remain. Furthermore, much of the literature to date has focused on polysaccharide or chitosan-based matrices rather than plant-protein matrices such as wheat gluten. Recent reviews of biopolymer-based biodegradable films point to the urgent need for novel functional materials that simultaneously achieve scalable producibility, safety compliance, mechanical robustness and active functionality (Dirpan *et al.* 2023).

In this context, metal–organic frameworks (MOFs), and in particular the zeolitic imidazolate framework-8 (ZIF-8), present a promising alternative. ZIF-8 offers a dodecahedral, zeolite-like crystalline structure built from Zn^{2+} ions and 2-methylimidazole ligands which provides high specific surface area, microporosity and excellent chemical/thermal stability (García-Palacín *et al.* 2020). More recently, applications of ZIF-8 in active packaging have been explored: for example, composite films based on gelatin/alginates loaded with ZIF-8 nanoparticles showed enhanced UV-light blocking, improved water resistance, lower water vapour permeability, and extended shelf-life of strawberries (Li *et al.* 2023). Also, PVA/ZIF-8@trans-cinnamaldehyde films demonstrated increased tensile strength by ~17%, improved moisture resistance and antimicrobial activity against Echerichia coli in spinach-leaf packaging studies (Hara *et al.* 2023). While a recent review highlights the potential of ZIFs in smart/active food packaging — noting advantages such as sustainability, functional tunability and sensor integration — it also emphasises that applications within protein-based film matrix remain under-explored (Sani *et al.* 2024).

Therefore, the present study aims to address these gaps by systematically investigating the incorporation of ZIF-8 within a wheat gluten-based edible film (GBEF) matrix. The specific objectives are: (1) to fabricate gluten-based edible films incorporating varying concentrations of ZIF-8 and evaluate their structural integrity, reproducibility and distribution of the MOF within the film matrix; and (2) to comprehensively assess the resulting films' physicochemical (thickness, WVTR), mechanical (tensile strength, elongation at break), rheological (film-forming solution behaviour), and biological (antibacterial) properties. By doing so, this work not only extends the application of ZIF-8 beyond polysaccharide or synthetic polymer matrix into a plant-protein framework, but it also provides insight into how MOF incorporation influences gluten film behaviour — thereby advancing active edible-film technologies toward safer, more functional and industrially viable food-packaging solutions.

MATERIALS AND METHOD

Materials

Commercial vital wheat gluten (VWG) with a moisture content of approximately 3% was obtained from a local food supplier in Bandung, Indonesia. All reagents used were of analytical grade, including ethanol (95%, Merck, Germany), glycerol (98%, Merck, Germany), ammonium hydroxide (NH_4OH, 6 N, Merck, Germany), zinc nitrate hexahydrate ($Zn(NO_3)_2 \cdot 6H_2O$, pro analysis grade, Sigma-Aldrich, Germany), 2-methylimidazole (mIm, 99%, Sigma-Aldrich, Germany), and methanol (MeOH, 99%, Merck, Germany). Bacterial strains of *Escherichia coli* and *Staphylococcus aureus* were obtained from the Bioprocess Laboratory, Politeknik Negeri Bandung, Indonesia. An acrylic casting mold (200 × 100 × 0.25 mm^3) used for film preparation was purchased from a local food-packaging supplier in Bandung, Indonesia.

Synthesis of ZIF-8 Crystal

ZIF-8 crystals were synthesized following a previously reported method with slight modifications (García-Palacín *et al.* 2020; Wang *et al.* 2023a). Briefly, 2.933 g of zinc nitrate hexahydrate ($Zn(NO_3)_2 \cdot 6H_2O$) was dissolved in 200 mL of methanol to prepare the first solution, while 6.489 g of 2-methylimidazole (mIm) was dissolved in 200 mL of methanol to prepare the second solution. The zinc nitrate solution was rapidly poured into the 2-methylimidazole solution under continuous stirring and maintained at room temperature for 30 minutes. The resulting suspension was centrifuged at 4500 rpm for 30 minutes, and the obtained white precipitate was washed twice with 50 mL of fresh methanol to remove unreacted residues. The purified ZIF-8 crystals were then dried overnight at room temperature to yield the final product.

Preparation of the Glu/Gly/ZIF-8 Edible Film

The preparation of gluten-based edible films incorporated with ZIF-8 was carried out with slight

modifications from previously reported methods (Jiang *et al.* 2023; Djenar *et al.* 2024b). Initially, 50 mL of 95% ethanol was heated to 75 °C for 2 min and subsequently mixed with 4.5 mL of glycerol under magnetic stirring at 200 rpm for 2 min. Then, 10 g of vital wheat gluten (VWG) was added to the ethanol–glycerol mixture and stirred for another 2 min. The temperature of the solution was then reduced to 60 ± 1 °C, followed by the addition of 8 mL of 6 N ammonium hydroxide (NH_4OH) and stirring for 3 min.

ZIF-8 powder was incorporated into the mixture at varying concentrations of 0.25%, 0.50%, 0.75%, and 1.00% (w/v) and stirred for 3 min to ensure uniform dispersion. Subsequently, 32 mL of distilled water was added, and the mixture was stirred for 30 min before being homogenized using an ultrasonic processor (Auguri Model LW 200D Digital Ultrasonic Cleaner, GuangDong GT Ultrasonic Co., Ltd., Shenzhen, China) at 50 °C for 10 min. The resulting Glu/Gly/ZIF-8 solution was then cast into molds and allowed to stand at room temperature for 30 min, followed by drying at 60 °C for 5 h to obtain the final films.

Antibacterial Activity Test of the Glu/Gly/ ZIF-8 Edible Film

The antibacterial activity of the Glu/Gly/ZIF-8 edible films was evaluated against Gram-negative (*Escherichia coli*) and Gram-positive (*Staphylococcus aureus*) bacteria using the disc diffusion method (Djenar *et al.* 2024b; Khashayary & Aarabi 2021). Briefly, 0.1 mL of bacterial suspension of either *E. coli* or *S. aureus* was uniformly spread onto sterile Petri dishes containing nutrient agar medium. Circular film samples (10 mm in diameter) were cut from the Glu/Gly/ZIF-8 films and sterilized under UV-LED light for 30 min prior to testing. The sterilized discs were aseptically placed on the inoculated agar surfaces and incubated at 37 °C for 72 h. Antibacterial activity was determined by measuring the diameter of the inhibition zone surrounding each film disc (in millimeters). Larger inhibition zones indicated stronger antibacterial performance (Djenar *et al.* 2024b; Azari *et al.* 2021; Motelica *et al.* 2021).

Measurement of Water Vapor Transmission Rate (WVTR)

The water vapor transmission rate (WVTR) of the Glu/Gly/ZIF-8 films was determined according to the ASTM E96–01 (1997) standard method (Djenar *et al.* 2024b). A permeation Petri dish (PPD) with a diameter of 60 mm containing 3 g of silica gel was sealed with the Glu/Gly/ZIF-8 film sample. The sealed PPD was then placed in a controlled chamber maintained at 25.1 °C and 77% relative humidity (RH) for 24 h. The dish was weighed before and after exposure to determine the amount of water vapor transmitted through the film.

The WVTR ($g \cdot m^{-2} \cdot 24\ h^{-1}$) was calculated using the following equation (1). (Djenar *et al.* 2024b; Cazón *et al.* 2022).

$$WVTR = \frac{(W - W_0)}{t \times A} \quad \ldots (1)$$

where W_0 is the initial weight of the PPD sealed with the Glu/Gly/ZIF-8 film (g), W is the final weight of the PPD after 24 h (g), t is the exposure time (h), and A is the surface area of the exposed film (m^2).

Measurement of Thickness

The thickness of each Glu/Gly/ZIF-8 film sample was measured five times at four randomly selected points using a screw micrometer (Model MDC-25M, Mitutoyo, Japan) (Djenar *et al.* 2024b; Wang *et al.* 2023b). Each film sample was placed on a fixed platform with an approximate spacing of ±50 mm along both length and width. The micrometer spindle was carefully adjusted to gently sandwich the film between the measuring surfaces. Thickness readings were recorded from the main scale and vernier scale, and the average value of all measurements was reported.

Measurement of Tensile Strength (TS) and Elongation at Break (EAB)

The tensile strength (TS) and elongation at break (EAB) of each Glu/Gly/ZIF-8 sample were measured in accordance with the ASTM D5034 standard using an Autograph Universal Testing Machine (AGX-V series, Shimadzu, Nakagyo-ku, Japan). Measurements were conducted in quintuplicate for each sample. Rectangular specimens with a cross-sectional area of 40 × 10 mm^2 were clamped at both ends and stretched until failure to determine the maximum applied force. The EAB was calculated using Equation (2) (Li *et al.* 2020).

$$\varepsilon = \frac{\Delta L}{L_0} \times 100\% \quad \ldots (2)$$

where ε is the elongation at break (%) of the Glu/Gly/ZIF-8 sample, ΔL is the change in length at break (mm), and L_0 (40 mm) is the initial gauge length of the specimen.

$$\delta = \frac{F\,\max}{A} \quad \ldots (3)$$

where σ is the tensile strength (N/m^2 or MPa), Fmax is the maximum applied force (N), and A is the cross-sectional area of the specimen (m^2) (Djenar *et al.* 2024b).

Material Characterization

The structural and chemical characteristics of the GBEF samples were investigated using Fourier-transform infrared (FTIR) spectroscopy (Bruker α II, Bruker GmbH, Mannheim, Germany) within the wavenumber range of 400–4000 cm^{-1} to identify functional groups and assess intermolecular interactions.

Surface wettability was determined through static water contact angle measurements. Contact angles were analyzed from captured droplet images using ImageJ software (National Institutes of Health, Bethesda, MD, USA).

The surface morphology and elemental distribution of the Glu/Gly/ZIF-8 samples were characterized by scanning electron microscopy coupled with energy-dispersive X-ray spectroscopy (SEM-EDS) at magnifications of 2000× and 5000× (Bruker GmbH, Mannheim, Germany).

RESULT AND DISSCUSION

Synthesis of ZIF-8

In this study, ZIF-8 was synthesized rapidly at room temperature, followed by a centrifugation process to complete the formation. The synthesized ZIF-8 was subsequently characterized qualitatively using FTIR spectroscopy to identify its functional groups, as shown in Figure 1(a) and 1(b).

Figure 1(a) presents the FTIR spectrum of the synthesized ZIF-8, showing characteristic absorption bands at 3132.40 cm^{-1} and 2927.94 cm^{-1}, which correspond to the aromatic and aliphatic C–H stretching vibrations of the imidazolate linker, respectively (Wang *et al.* 2023a). These results are consistent with the findings shown in Figure 1(b), where the typical functional groups of ZIF-8 appear at approximately 3135 and 2929 cm^{-1} (Azam *et al.* 2020). Additional absorption bands were observed at 1583.56 cm^{-1}, 1143.79 cm^{-1}, and 993 cm^{-1}, corresponding to the C=N and C–N stretching vibrations of the imidazolate framework. Peaks at 1307.74 cm^{-1}, 1421.54 cm^{-1}, 754.17 cm^{-1}, and 690.52 cm^{-1} were attributed to the imidazole ring vibrations, while the absorption band at 420.49 cm^{-1} confirmed the presence of Zn–N stretching, characteristic of the ZIF-8 structure (Wang *et al.* 2023a; Azam *et al.* 2020). These results confirm that ZIF-8 was successfully synthesized and is suitable for subsequent incorporation into the GBEF matrix.

Zeolite imidazolate framework-8 (ZIF-8) is a crystalline member of the metal–organic frameworks (MOFs) family. The formation of its porous crystalline structure is strongly influenced by the synthesis method and the solvent employed. In this study, methanol was selected as the solvent because it is a protic solvent capable of hydrogen bonding, which facilitates the deprotonation of the organic ligand 2-methylimidazole (HmIm), as illustrated in Figure 2.

Methanol's low viscosity promotes efficient diffusion of reactants, allowing Zn^{2+} and mIm^{-} ions to readily interact and form ZIF-8 crystals. The molecular size of methanol is comparable to the pore aperture of the ZIF-8 sodalite framework, enabling temporary incorporation of methanol molecules within the pores during crystallization. These molecules are subsequently released without disrupting the overall framework, although minor structural defects may form (Tezerjani *et al.* 2021).

The synthesis reaction of ZIF-8 can be represented as follows equation (4) (García-Palacín *et al.* 2020).

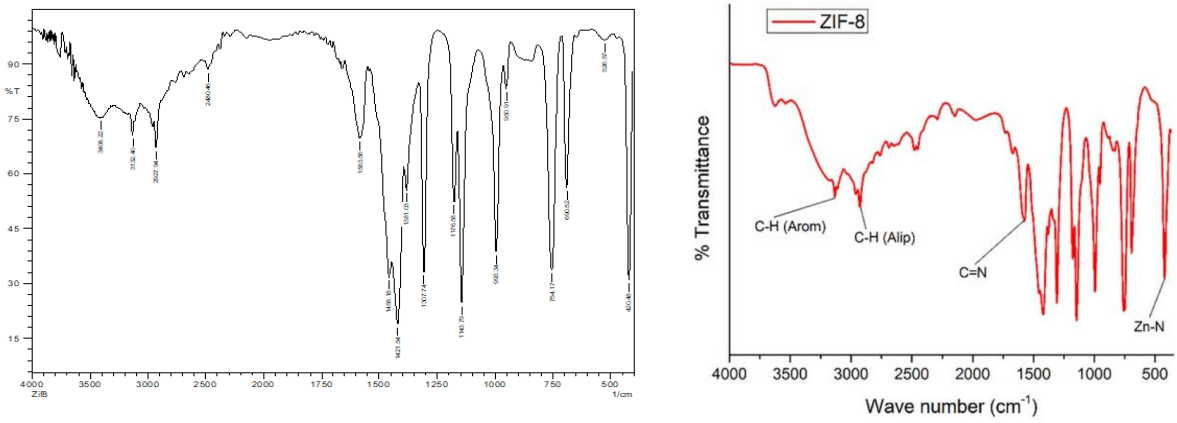

(a) (b)

Figure 1. (a) FTIR spectra of synthesized ZIF-8 and (b) FTIR spectra of ZIF-8 (Azam *et al.* 2020)

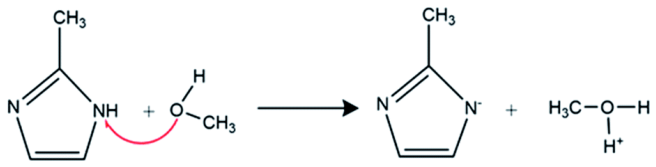

Figure 2. Reaction scheme of HmIm deprotonation in methanol (Tezerjani *et al.* 2021)

$$Zn(NO_3)_2 \times 6H_2O + 2C_4H_6N_2 \rightarrow Zn(C_4H_5N_2)_2 + 2H^+ + 2NO_3^- + 6H_2O \quad ...(4)$$

During crystallization, the pH of the solution decreases due to the formation of nitric acid, which moderates the transformation rate of mIm. The synthesis process is conducted at room temperature under alkaline conditions to prevent excessive acidification, as nitric acid is corrosive and could compromise the stability of the organic phase. Further optimization of washing frequency and drying temperature is recommended to improve the sustainability and reproducibility of ZIF-8 synthesis (García-Palacín *et al.* 2020).

Glu/Gly/ZIF-8 EF Formulation

The Glu/Gly/ZIF-8 edible film (EF) was prepared from a mixture of vital wheat gluten (VWG), 96% ethanol, glycerol, 20% ammonium hydroxide, ZIF-8, and distilled water. Ethanol served as a solvent for gluten, while glycerol was used as a plasticizer. Ammonium hydroxide was added to increase the pH, promoting an alkaline environment that enhances gluten solubility. ZIF-8 was incorporated at concentrations of 0.25%, 0.50%, 0.75%, and 1% (w/w), resulting in a viscous, yellowish film-forming solution (Wang *et al.* 2023a).

To reduce gas content and accelerate homogenization, the mixture underwent sonication, which disrupted intermolecular bonds within the gluten-based matrix and facilitated the formation of nanoscale ZIF-8 dispersions (Jiang *et al.* 2023). The film-forming solution was subsequently cast and dried in an oven at 60 °C. The resulting Glu/Gly/ZIF-8 edible film is shown in Figure 3.

Based on Figure 3, the incorporation of ZIF-8 at various concentrations did not produce a noticeable change in the visual appearance of the edible films, all of which exhibited a uniform pale-yellow color. This coloration originates from gluten, which contains natural yellow carotenoid pigments derived from wheat grains (Masibi *et al.* 2022; Vida *et al.* 2022). At higher ZIF-8 loadings (0.75% and 1%), the presence of some course ZIF-8 particles was observed, likely resulting from particle agglomeration and uneven dispersion during the casting process. Similar phenomena have been reported in chitosan/sodium alginate (CS/SA) composite films incorporating QDs@ZIF-8 nanoparticles, where increased nanoparticle content led to rougher film surfaces and higher water contact angles (Wang *et al.* 2023b).

The incorporation of glycerol, a low-molecular-weight hydrophilic compound, facilitates its integration into the gluten network, where it forms hydrogen bonds with reactive groups on amino acid residues. This interaction reduces intermolecular bonding among gluten proteins, increases the spacing between protein chains, and decreases direct chain–chain interactions (Kłosok *et al.* 2021). As a result, glycerol weakens intermolecular forces and lowers the glass transition temperature (Tg) of gluten, thereby enhancing the mobility of the polymer chains (Abdullah-Al-Rahim 2021). The addition of 5% glycerol as a plasticizer in the GBEF formulation reduces the processing temperature and yields a more flexible, less rigid film with improved stretchability (Wu *et al.* 2024).

The surface morphology of the Glu/Gly/ZIF-8 films is further influenced by the incorporation of ZIF-8 nanoparticles. Increasing ZIF-8 concentration leads to greater surface roughness due to nanoparticle aggregation and their uneven distribution within the polymer matrix. Scanning electron microscopy (SEM) observations confirmed that films containing ZIF-8 exhibited a rougher surface compared to those without ZIF-8, which can consequently affect barrier properties and adhesion behavior (Lee *et al.* 2019)

Characterization of Glu/Gly/ZIF-8 Edible Film Based on Rheological Properties and WVTR

This characterization was conducted to evaluate (1) the relationship between tensile strength (TS) and elongation at break (EAB) of Glu/Gly/ZIF-8 edible films (EFs) containing various ZIF-8 concentrations,

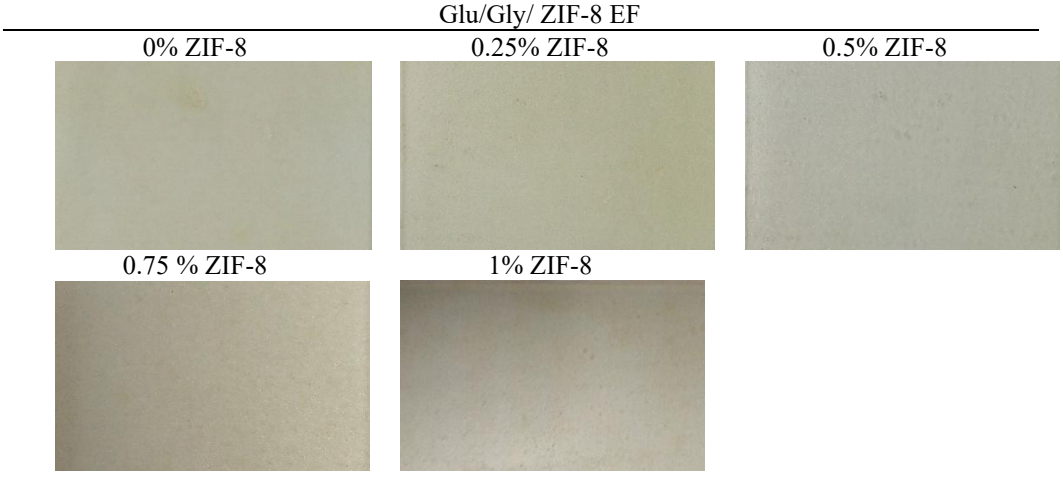

Figure 3. Glu/Gly/ZIF-8 edible films (EF) prepared with different ZIF-8 concentrations (0.25%, 0.50%, 0.75%, and 1.00%)

and (2) the barrier performance of the films as indicated by their water vapor transmission rate (WVTR). The results of these measurements are summarized in Table 1.

Water Vapor Transmission Rate (WVTR)

The water vapor transmission rate (WVTR) is a measure of the rate at which water vapor permeates through a film layer. It reflects the film's capacity to control moisture transfer between the external environment and the packaged food (Zhao *et al.* 2020). A lower WVTR indicates superior barrier performance, as the film is more effective in preventing moisture migration, thereby extending the shelf life of packaged products (Wang *et al.* 2023b). The WVTR values obtained for Glu/Gly/ZIF-8 edible films with varying ZIF-8 concentrations are presented in Figure 4.

In a previous study, GBEF films incorporated with beef extract (BE) and ZnO nanoparticles (ZnONPs, 0.1–0.4%) exhibited WVTR values ranging from 5.0069 to 6.8677 g/m²/24 h (Djenar *et al.* 2024b). As shown in Figure 4, the addition of ZIF-8 to the Glu/Gly edible film resulted in substantially lower WVTR values. The control film (0% ZIF-8) exhibited a WVTR of 1.4560 g/m²/24 h, while films containing ZIF-8 at various concentrations showed reduced WVTR values ranging from 1.0848 to 1.4530 g/m²/24 h.

The reduction in WVTR is attributed to chemical cross-linking interactions between the nanosized, porous ZIF-8 particles and the functional groups of the gluten/glycerol matrix. These interactions include hydrogen bonding between hydroxyl groups in glycerol and gluten, as well as electrostatic interactions between Zn^{2+} ions and oxygen atoms of gluten molecules. Such bonding promotes a denser, more compact film structure and enhances interfacial compatibility between the hydrophilic glycerol and hydrophobic gluten components. Consequently, the Glu/Gly/ZIF-8 edible films exhibit excellent barrier performance against H_2O, CO_2, and O_2, as illustrated in Figure 5 (Geng *et al.* 2023). This observation aligns with previous findings that the incorporation of rigid and hydrophobic ZIF-8 nanoparticles reduces water vapor diffusion through polymer matrices, thereby lowering WVTR (Lee *et al.* 2019).

Although ZIF-8 possesses high intrinsic porosity, its effect on gas transport is not solely governed by pore volume but rather by pore size distribution, connectivity, and interfacial interactions with the polymer matrix. ZIF-8 features uniform micropores with apertures of approximately 3.4 Å, comparable to or smaller than the kinetic diameters of gas molecules such as H_2O (2.65 Å), CO_2 (3.3 Å), and O_2 (3.46 Å). When dispersed within the gluten/glycerol network, these micropores act as molecular sieves, selectively adsorbing smaller gas molecules while restricting the passage of larger ones. Moreover, the interfacial

Table 1. Rheological and Barrier Properties of Glu/Gly/ZIF-8 Edible Films (EFs) in Compliance with Japanese Industrial Standards (JIS)

Functional Property	Unit	Composition of ZIF-8					JIS
		0.00%	0.25%	0.50%	0.75%	1.00%	
WVTR	g/m²/24 h	1.4560	1.3192	1.0848	1.1020	1.4530	≤10
Thickness	Mm	0.18	0.20	0.26	0.20	0.23	≤0.25
EAB	%	416.94	382.83	251.75	290.92	211.86	70 (*minimum*)
TS	MPa	45.660	43.882	32.178	60.583	49.682	0.3 (*minimum*)

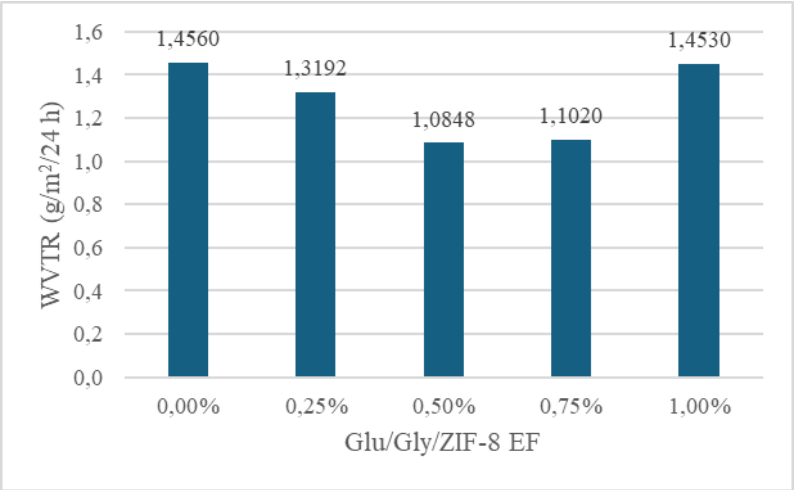

Figure 4. Water vapor transmission rate (WVTR) of Glu/Gly/ZIF-8 edible films with different ZIF-8 concentrations

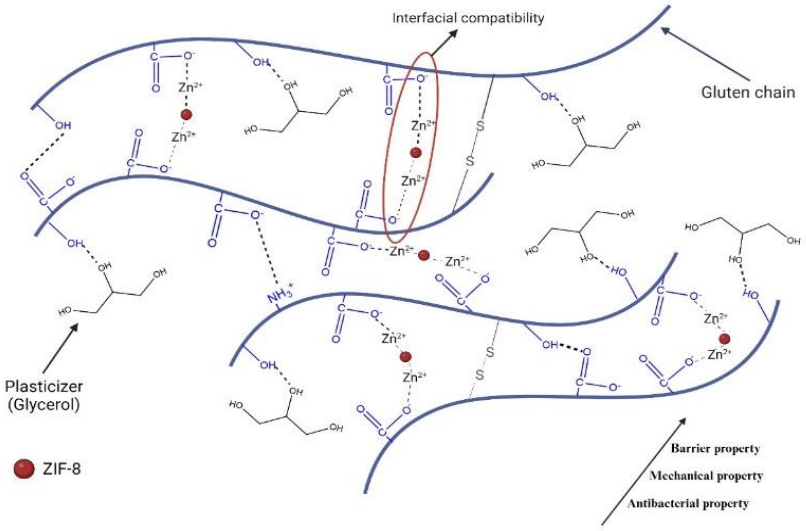

Figure 5. Schematic illustration of the structural network and interfacial interactions between gluten, glycerol, and ZIF-8 within the Glu/Gly/ZIF-8 edible film (EF)

cross-linking between ZIF-8 and the polymer chains reduces the effective free volume of the matrix, further hindering gas diffusion. Hence, although ZIF-8 is highly porous in isolation, its incorporation into a continuous polymer network effectively reduces gas permeability by imposing tortuous and size-selective diffusion pathways (Liu *et al.* 2019; Masibi *et al.* 2022). Nevertheless, while the observed decrease in gas transmission supports this mechanism, quantitative evaluation of gas absorption, retention, and diffusion selectivity is necessary to substantiate the proposed barrier behavior.

Physical and Mechanical Properties

Film thickness is an important parameter specified by the Japanese Industrial Standards (JIS), as it directly influences the suitability of a film for food packaging applications. Thickness affects not only the transmission of water vapor, gases, and volatile compounds but also the mechanical properties, including tensile strength and elongation at break (Karnwal *et al.* 2025). The thickness measurements of the Glu/Gly/ZIF-8 edible films are presented in Figure 6.

Figure 6 shows that the thickness of Glu/Gly/ZIF-8 edible films (EFs) with varying ZIF-8 concentrations generally complies with JIS standards (≤0.25 mm), except for Glu/Gly/ZIF-8 0.5%. In the control film without ZIF-8, the thickness was 0.18 mm, whereas the addition of ZIF-8 increased it to 0.20–0.26 mm. This increase is attributed to cross-linking between Zn^{2+} ions from ZIF-8 and the $–NH_2$ groups of gluten, forming a ZIF-8 network that integrates closely with the polymer matrix (Djenar *et al.* 2024b; Geng *et al.* 2023; Azari *et al.* 2021; Xing *et al.* 2019).

The observed fluctuations in film thickness are also influenced by the casting process, which can produce surface roughness. Similar trends have been reported in previous studies: the incorporation of QDs@ZIF-8 into chitosan/sodium alginate-based nanocomposite films led to increased thickness with higher nanoparticle concentrations (Wang *et al.* 2023b). Likewise, the addition of APG@ZIF-8 to composite films resulted in a notable thickness increase, ranging from 0.097 to 0.157 mm, compared to 0.059 mm for films without ZIF-8 (Wang *et al.* 2023a).

The incorporation of Zeolitic Imidazolate Framework-8 (ZIF-8) into composite packaging materials can influence film thickness. However, research indicates that the addition of ZIF-8 to polymer matrix, such as polyvinyl alcohol (PVA) and starch blends, produces only minor variations in thickness. For instance, one study reported that the thickness of PVA/starch/methylcellulose films remained relatively stable across different ZIF-8 concentrations, ranging from approximately 97.1 µm to 98.3 µm (Lee *et al.* 2019). Moreover, while maintaining minimal changes in thickness, ZIF-8 increases surface roughness and can enhance mechanical properties. These characteristics make ZIF-8 an effective additive for developing advanced packaging materials that retain structural integrity without compromising flexibility.

Tensile strength (TS) is a key rheological property of nanocomposite films, reflecting the cohesive and elastic mechanical integrity of the gluten network (Djenar *et al.* 2021). The TS test was performed to assess the mechanical properties of Glu/Gly/ZIF-8 edible films (EFs). The results of this analysis are presented in Figure 7.

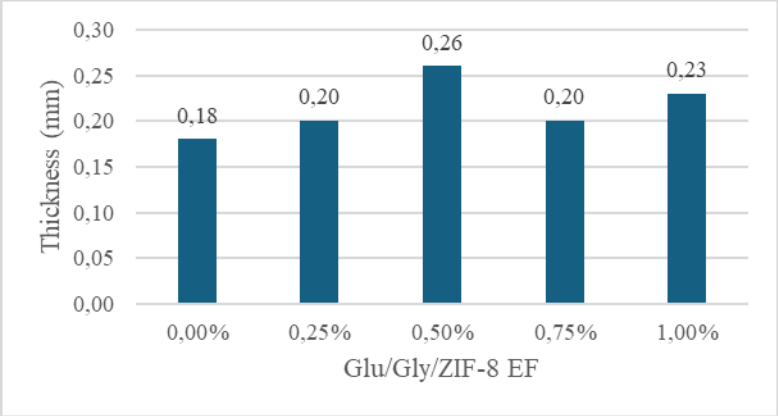

Figure 6. Thickness of Glu/Gly/ZIF-8 edible films (EFs) prepared with varying concentrations of ZIF-8

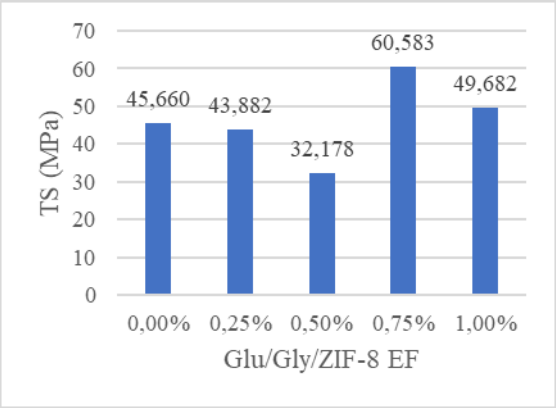

Figure 7. Tensile strength (TS) of Glu/Gly/ZIF-8 edible films (EFs) prepared with varying ZIF-8 concentrations

GBEF incorporated with ZnO nanoparticles (0.1–0.4%) exhibited a tensile strength (TS) ranging from 34.45 to 45.39 MPa (Djenar *et al.* 2024b). In this study, Glu/Gly edible films (EFs) with varying ZIF-8 concentrations showed a broader TS range of 32.178–60.583 MPa (Figure 7). The TS of the film without ZIF-8 was 45.66 MPa. With low ZIF-8 loadings (0.25% and 0.50%), TS decreased to 43.882 MPa and 32.178 MPa, respectively, likely due to insufficient ZIF-8 dispersion, which disrupted matrix homogeneity. Increasing ZIF-8 to 0.75% significantly enhanced TS to 60.583 MPa, attributed to improved intermolecular interactions—including hydrogen and chemical bonds—between the rigid ZIF-8 nanoparticles and the gluten/glycerol (Glu/Gly) matrix. However, at 1% ZIF-8, TS decreased to 49.682 MPa, likely due to nanoparticle agglomeration and increased porosity, which reduced matrix homogeneity (Lee *et al.* 2019).

Previous studies support these trends: QD@ZIF-8 addition to chitosan/sodium alginate (CS/SA) films increased TS from 25.5 MPa to 28.6, 30.3, and 27.8 MPa with 0.1%, 0.25%, and 0.5% loadings, respectively (Wang *et al.* 2023b). Similarly, Cur-ZIF-8 incorporation in chitosan/zein (CS/Zein) films improved TS and elongation at break (EAB) from 22.7 ± 1.1 MPa and 3.5 ± 0.5% to 24.7 ± 2.0 MPa and 42.2 ± 2.1%, respectively (Geng *et al.* 2023).

The incorporation of Zeolitic Imidazolate Framework-8 (ZIF-8) into composite food packaging significantly enhances tensile strength by reinforcing the polymer matrix and improving stress distribution under load. For example, polyvinyl alcohol (PVA) films embedded with ZIF-8 nanoparticles exhibited a 17% increase in tensile strength compared to control films, demonstrating improved mechanical performance and suitability for low load-bearing applications such as food packaging (Hara *et al.* 2023). The enhancement is attributed to the rigid ZIF-8 nanoparticles acting as nanoreinforcements and forming effective interactions with polymer chains, resulting in more stable, flexible, and durable composites (Bora *et al.* 2024). Uniform dispersion and compatibility of ZIF-8 within the polymer matrix are critical for maximizing these mechanical benefits (Lee *et al.* 2019). In addition to improving tensile strength, ZIF-8 incorporation can confer functional advantages such as antimicrobial activity, making it a promising additive for advanced food packaging applications.

The elongation at break (EAB) percentage quantitatively reflects the stretchability of the GBEF matrix and is closely associated with the degree of

plasticization. The EAB values of GBEF containing ZIF-8 at various concentrations are presented in Figure 8.

Figure 8 shows that Glu/Gly/ZIF-8 edible films (EFs) with varying ZIF-8 concentrations maintain elongation at break (EAB) values above the JIS minimum requirement of 70%. The EAB of the control film (0% ZIF-8) was 416.94%, whereas films containing ZIF-8 exhibited lower and fluctuating EAB values, ranging from 211.86% to 382.83%. Increasing ZIF-8 concentration generally led to a decrease in EAB, indicating reduced film flexibility. This reduction is attributed to the reinforcement of the gluten polymer network by ZIF-8, which strengthens chain interactions without steric hindrance, limiting chain mobility (Lee *et al.* 2019).

The observed decrease in EAB aligns with previous studies showing that the elongation of composite films decreases with higher concentrations of QD@ZIF-8 in chitosan/sodium alginate (CS/SA) films (Wang *et al.* 2023b) and APG@ZIF-8 in propolis-gelatin films (EAB decreased from 36.84% to 14.26%). Conversely, the addition of Cur-ZIF-8 to chitosan/zein (CS/Zein) films increased EAB from 3.5 ± 0.5% to 42.2 ± 2.1%, due to improved interfacial compatibility between hydrophilic and hydrophobic polymer components (Geng *et al.* 2023). For comparison, GBEF films containing 0.1–0.4% ZnO nanoparticles exhibited EAB values of 205.83–252.18% (Djenar *et al.* 2024b). In this study, the addition of 0.25–1.00% ZIF-8 resulted in EAB values of 211.86–382.83%, demonstrating that ZIF-8 can maintain relatively high flexibility while enhancing mechanical strength.

The incorporation of Zeolitic Imidazolate Framework-8 (ZIF-8) into composite food packaging materials significantly affects elongation at break (EAB), a key indicator of ductility and flexibility. Studies have shown that adding ZIF-8 to polymer matrices, such as PVA/starch/methyl cellulose films, can reduce EAB as ZIF-8 content increases. This trend indicates that while ZIF-8 improves tensile strength, the rigid nature of its nanoparticles restricts polymer chain mobility, thereby limiting the material's ability to stretch before failure (Lee *et al.* 2019). The mechanical behavior of such composites often involves a trade-off between strength and flexibility: enhanced structural reinforcement from ZIF-8 comes at the cost of reduced ductility. For example, composites with higher ZIF-8 concentrations exhibited lower EAB values compared to formulations with minimal or no ZIF-8, demonstrating that increased rigidity can constrain the polymer network and limit elongation (Hu *et al.* 2024).

In this study, the relationship between tensile strength (TS) and elongation at break (EAB) is strongly influenced by both the base ingredients of the edible film and the properties of the added components forming the composite. TS and EAB are primarily determined by the distribution and density of intermolecular and intramolecular interactions within the film's structural network, which in turn depend on the arrangement and orientation of polymer chains (Wan *et al.* 2018). These parameters are essential for evaluating the mechanical performance of edible or biodegradable nanocomposite films, particularly in preventing product damage, maintaining food quality, and serving as protective coatings for fruits during transportation and storage (Geng *et al.* 2023; Zhou *et al.* 2019). The Glu/Gly/ZIF-8 EF nanocomposite demonstrates potential for expanding the applications of protein/polymer composites in the agricultural and food industries (Geng *et al.* 2023; Wang *et al.* 2023b).

Measurement of Static Water Contact Angle

Hydrophilicity testing is important to assess the durability and surface behavior of biodegradable composite films. In this study, the wettability of Glu/Gly/ZIF-8 edible films (EFs) was measured using the water contact angle (WCA) method (Wang *et al.* 2023b). When the water contact angle exceeds 90°, the film is considered hydrophobic (Wang *et al.* 2023a). As shown in Figure 9, Glu/Gly/ZIF-8 EFs with varying ZIF-8 concentrations exhibited WCA values between 34.959° and 59.238°, indicating that the films remain hydrophilic since all angles were

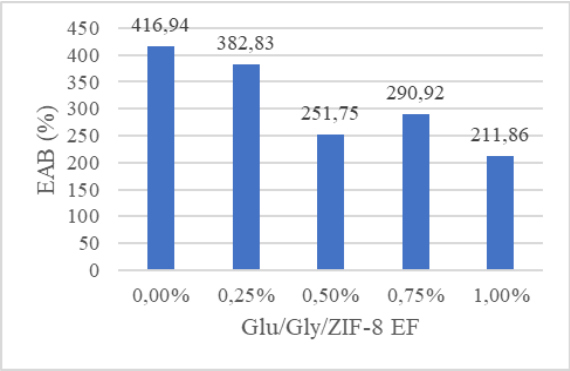

Figure 8. Elongation at Break (EAB) of Glu/Gly/ZIF-8 edible films with varying ZIF-8 concentrations

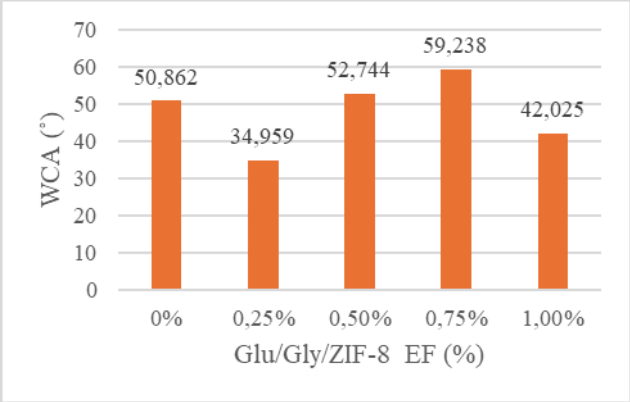

Figure 9. Water contact angle of Glu/Gly/ZIF-8 EF with varying concentrations of ZIF-8

below 90°. This hydrophilic nature is primarily due to the presence of glycerol, which contains hydroxyl groups that increase the film's affinity for water and make it more hygroscopic (Chen *et al.* 2021).

Previous studies have reported that the WCA of gluten-based nanofibrous films decreases with increasing concentrations of glycerol monolaurate (GML), from 48.5° to 33.3°, demonstrating enhanced surface hydrophilicity (Zhang *et al.* 2020). Similarly, the hydrophilicity of Glu/Gly/ZIF-8 EFs may arise from the increased surface energy of gluten interacting with glycerol through hydrogen bonding (Channab *et al.* 2024). A more hydrophilic surface also improves the dispersion of water and incorporated active compounds, which can enhance functional performance in food packaging applications (Zhu *et al.* 2019).

Interestingly, at ZIF-8 concentrations of 0.50% and 0.75%, the WCA increased to 52.744° and 59.238°, respectively, though still below 90°. This slight increase suggests that hydrogen bonding between ZIF-8 and the gluten matrix, along with the superhydrophobic structure of ZIF-8, contributes to reduced surface wettability (Wang *et al.* 2023b). The incorporation of ZIF-8 has been reported to alter the hydrophilic/hydrophobic balance of polymer-based composites, with higher concentrations typically increasing WCA values due to changes in surface morphology and roughness (Masibi *et al.* 2022; Shen *et al.* 2022). According to the Cassie–Baxter model, the rougher surface created by ZIF-8 nanoparticles can trap air pockets beneath water droplets, leading to higher contact angles and decreased wettability.

ZIF-8 interacts with the polymer matrix and influences the distribution and orientation of polymer chains, particularly at the film surface. This interaction promotes a more ordered molecular arrangement that favors hydrophobic characteristics. Moreover, hydrogen bonding between ZIF-8 and functional groups within the polymer network can modify surface energy and reduce water affinity. The resulting increase in water contact angle enhances the film's moisture barrier performance, making it more effective in limiting water vapor transmission. Such improvement is especially advantageous for food packaging applications, where moisture control is critical to maintaining product quality and extending shelf life.

Antibacterial Activities of the Glu/Gly/ ZIF-8 EF

The antibacterial activity of Glu/Gly/ZIF-8 edible films (EFs) was evaluated based on the diameter of the inhibition zone against *Escherichia coli* (Gram-negative) and *Staphylococcus aureus* (Gram-positive). The results are shown in Figures 10–12.

Both ZIF-8 alone and Glu/Gly/ZIF-8 EFs exhibited inhibitory effects on bacterial growth across all ZIF-8 concentrations. However, the inhibition zones were consistently larger for *S. aureus* (25–34 mm) than for *E. coli* (25–26 mm). This difference is attributed to structural variations between the two bacterial types—*S. aureus* possesses a thicker peptidoglycan layer but is more chemically sensitive, while *E. coli* has a relatively impermeable outer lipid membrane that limits antimicrobial penetration (Shen *et al.* 2020).

As shown in Figure 10, ZIF-8 in powder form and dissolved in methanol demonstrated notable antibacterial effects, producing inhibition zones of 19 mm and 10 mm against *S. aureus*, and 20 mm and 10 mm against *E. coli*, respectively. These findings confirm that metal–organic frameworks (MOFs) such as ZIF-8 exert antibacterial activity primarily through the release of Zn^{2+} ions (Wang *et al.* 2023a; Ahmad *et al.* 2020; Kermanshahi & Akhbari 2024). Furthermore, the incorporation of ZIF-8 into the GBEF matrix enhanced antibacterial efficacy compared to ZIF-8 alone, indicating synergistic interactions between ZIF-8 and the polymeric components. Similar behavior was observed in APG@ZIF-8 composite films, which exhibited strong antibacterial effects against both Gram-positive and Gram-negative bacteria (Wang *et al.* 2023a).

ZIF-8 exhibits antibacterial properties primarily through two mechanisms. First, the generation of reactive oxygen species (ROS) such as hydrogen peroxide (H_2O_2), which induces oxidative stress and damages bacterial cell components (Shen *et al.*

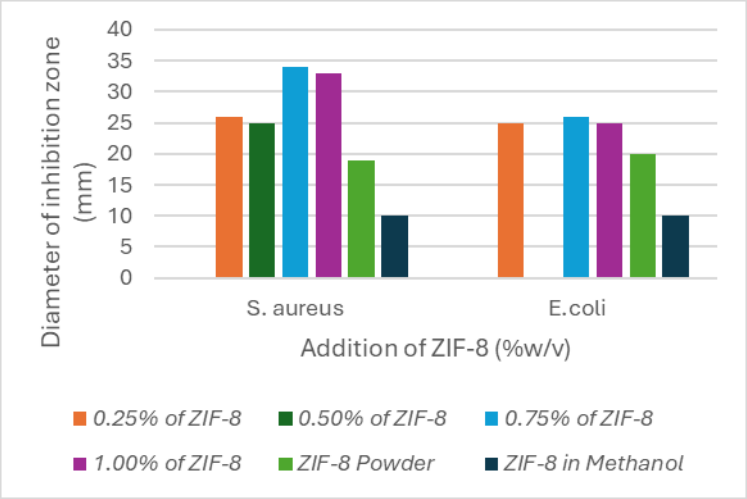

Figure 10. Diameter of inhibition zone of the Glu/Gly/ZIF-8 EF

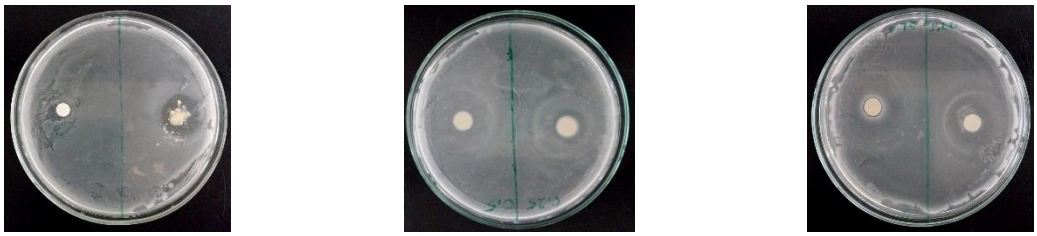

(a) (b) (c)

Figure 11. Antibacterial activity of (a) ZIF-8, (b) Glu/Gly/0.25% ZIF-8 EF and Glu/Gly/0.50% ZIF-8 EF, and (c) Glu/Gly/0.75% ZIF-8 EF and Glu/Gly/1% ZIF-8 EF against *E. coli*

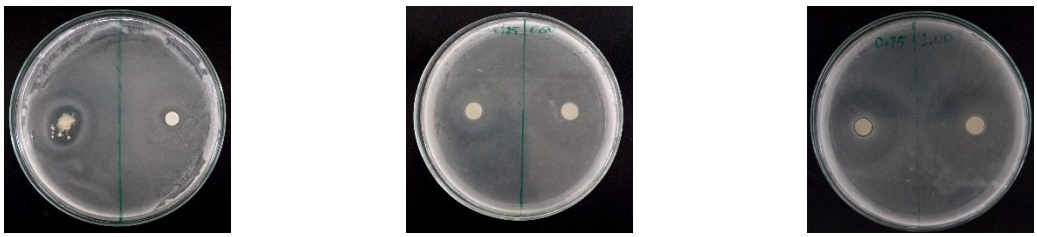

(a) (b) (c)

Figure 12. Antibacterial activity of (a) ZIF-8, (b) Glu/Gly/0.25% ZIF-8 EF and Glu/Gly/0.50% ZIF-8 EF, and (c) Glu/Gly/0.75% ZIF-8 EF and Glu/Gly/1% ZIF-8 EF against *S. aureus*

2022). Second, the gradual release of Zn^{2+} ions, which bind to bacterial membrane proteins, disrupt cell integrity, and inhibit enzymatic functions (Shen *et al.* 2022; Kermanshahi & Akhbari 2024). The balance between these mechanisms contributes to the broad-spectrum antibacterial performance of ZIF-8-based materials. Moreover, combining ZIF-8 with other antimicrobial nanomaterials, such as silver nanoparticles (AgNPs), has been shown to enhance antibacterial efficacy through synergistic effects, offering potential for advanced multifunctional food packaging systems (Makhetha *et al.* 2020).

FTIR Analysis

Fourier-transform infrared (FTIR) spectroscopy was performed to identify functional groups and molecular interactions in the Glu/Gly/ZIF-8 edible film (EF) matrix. The analysis focused on Glu/Gly/0.25% ZIF-8 EF, Glu/Gly/0.75% ZIF-8 EF, ZIF-8, and vital wheat gluten (VWG). The FTIR spectra (Figure 13) showed that the four samples exhibited similar spectral patterns, indicating the presence of comparable chemical functionalities. The main absorption bands of Glu/Gly/0.25% and Glu/Gly/0.75% ZIF-8 EFs, compared with VWG and ZIF-8, are summarized in Table 2.

Figure 13 and Table 2 show characteristic absorption peaks at 3408.22 cm^{-1} and 2926.01 cm^{-1}

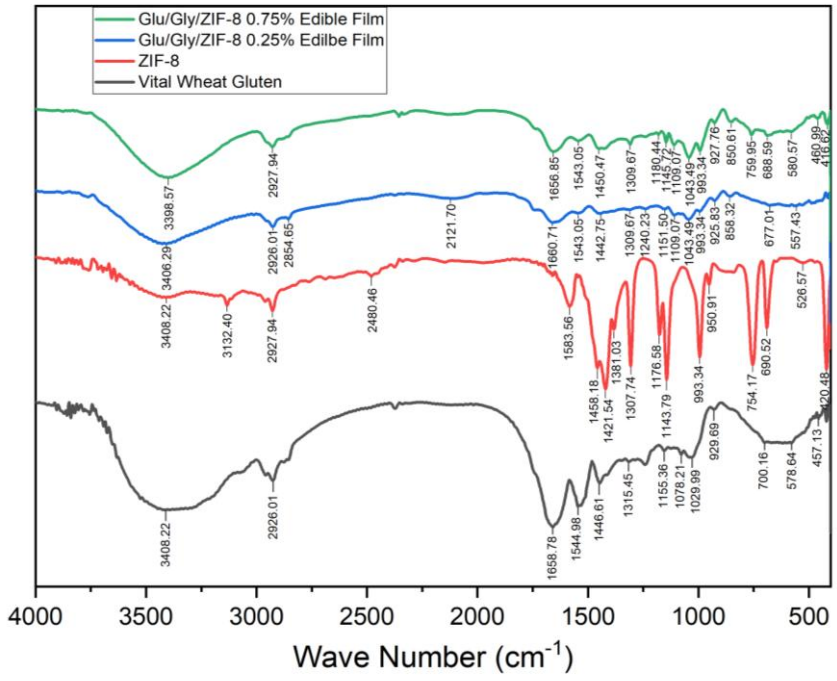

Figure 13. FTIR spectra of the constituent materials (VWG and ZIF-8) and Glu/Gly/ZIF-8 edible films at different ZIF-8 concentrations

Table 2. FTIR absorption bands of constituent materials and Glu/Gly/ZIF-8 edible films at different ZIF-8 concentrations

Material	Wavenumber (cm^{-1})									Ref.
	N-H	C-H	imidazole ring	Amide I			Amide II	Amide III	Zn-N	
				α-helix	β-*sheet*	β-*turns*	NH bending and CN	NH bending and CN		
Vital wheat gluten	3408.22	2926.01	-	1658.79	-	-	1544.96	1276.88	-	
ZIF-8		2927.94	3132.40; 1421.54; 754.17; 690.52	-	-	-	-	-	420.48	[29], [18]
Glu/Gly/ZIF-8 0.25% EF	3406.29	2926.01	677.01	1660.71	-	-	1543.05	-	-	
Glu/Gly/ZIF-8 0.75% EF	3398.57	2927.94	759.95; 688.59	1656.85	-	-	1543.05	-	416.62	

corresponding to N–H and C–H stretching, respectively; amide I (α-helix) at 1658.78 cm^{-1}; amide II at 1544.96 cm^{-1}; and amide III at 1276.88 cm^{-1} (Djenar *et al.* 2024b; Djenar *et al.* 2021; Krekora & Nawrocka 2022). These peaks confirm the presence of VWG functional groups within the Glu/Gly/ZIF-8 EF.

The incorporation of ZIF-8 into the Glu/Gly matrix induced several spectral changes. First, the amide III band disappeared, indicating alterations in the secondary protein structure. Second, the N–H stretching peak shifted from 3408.22 cm^{-1} to 3406.29 cm^{-1} and 3398.57 cm^{-1} for Glu/Gly/0.25% and Glu/Gly/0.75% ZIF-8 EFs, respectively. The C–H stretching peak also shifted slightly from 2926.01 cm^{-1} to 2927 cm^{-1}, while the amide I (α-helix) band shifted from 1658.79 cm^{-1} to 1660.71 cm^{-1} and 1656.85 cm^{-1}, respectively. These spectral shifts indicate the formation of intermolecular hydrogen bonds between the Glu/Gly matrix and ZIF-8 nanoparticles, with the degree of interaction increasing alongside ZIF-8 concentration.

The characteristic peaks of ZIF-8 were also observed in the composite films. In Glu/Gly/0.75% ZIF-8 EF, absorption bands appeared at 2927.94 cm^{-1} (aliphatic C–H stretching in the imidazolate group), 759.95 cm^{-1} and 688.59 cm^{-1} (imidazole ring vibrations), and 416.62 cm^{-1} (Zn–N stretching)

(Wang *et al.* 2023a; Azam *et al.* 2020; Lee *et al.* 2019). In contrast, Glu/Gly/0.25% ZIF-8 EF exhibited only two main ZIF-8-related bands: 2926.01 cm^{-1} (aliphatic C–H) and 677.01 cm^{-1} (imidazole ring). These results confirm that ZIF-8 is successfully embedded within the Glu/Gly matrix through physical blending rather than chemical reaction. The presence of ZIF-8 contributes to enhanced rheological, physicochemical, and antibacterial properties of the composite film (Djenar *et al.* 2024b).

Previous studies have also reported that the incorporation of ZIF-8 into biopolymer films modifies structural and thermal characteristics. Increasing ZIF-8 content promotes hydrogen bonding between the filler and polymer matrix, increasing bond polarization and intensifying FTIR absorption peaks (Lee *et al.* 2019; Caamaño *et al.* 2023). Furthermore, ZIF-8 addition can reduce nanoparticle agglomeration, improve matrix compatibility, and enhance thermal stability, as evidenced by scanning electron microscopy (SEM), atomic force microscopy (AFM), and thermogravimetric analysis (TGA) (Lee *et al.* 2019; Caamaño *et al.* 2023).

Similarly, in poly (vinyl alcohol) (PVA)-based films, FTIR analysis has shown that ZIF-8 incorporation shifts hydroxyl (O–H) stretching vibrations to higher frequencies, indicating stronger hydrogen bonding between PVA and ZIF-8. The imidazole ring in ZIF-8 provides good chemical affinity and compatibility with organic polymer matrices. Increasing ZIF-8 concentration leads to narrower and more intense absorption bands, reflecting enhanced molecular interactions. Characteristic absorption peaks of ZIF-8 include C–H stretching near 2937–2935 cm^{-1}, C=O stretching at 1722 cm^{-1}, C–H bending at 1428 cm^{-1}, C–C stretching at 1264 cm^{-1}, and C–O stretching near 1046 cm^{-1} (Lee *et al.* 2019).

Overall, FTIR analysis confirms that ZIF-8 was successfully incorporated into the Glu/Gly edible film matrix without forming new chemical compounds, indicating a physical blending process supported by hydrogen bonding and intermolecular interactions. The observed shifts in characteristic absorption peaks, particularly those associated with amide and hydroxyl groups, demonstrate that ZIF-8 alters the molecular arrangement and strengthens the interaction within the composite network. These modifications contribute to improved compatibility between ZIF-8 and the gluten–glycerol matrix, which enhances the film's mechanical integrity, physicochemical stability, and antibacterial functionality. The FTIR findings therefore support the role of ZIF-8 as an effective reinforcing agent that optimizes the structural and functional performance of Glu/Gly/ZIF-8 edible films for potential food packaging applications.

SEM-EDS Characterization

SEM analysis of Glu/Gly/0.75% ZIF-8 EF revealed the surface morphology and topography at magnifications of 2000× and 5000× (Figures 14 and 15).

The microstructure exhibited a relatively smooth surface, with ZIF-8 particles clearly visible and ranging in size from 63 nm to 3.04 μm (Figure 14b). This broad particle size distribution is attributed to the room-temperature synthesis without variations in time or temperature, and without prior optimization of methanol content. Previous studies have shown that synthesis parameters, including reaction time, material mole ratio, and pH, significantly influence ZIF-8 particle size and crystallinity, while low methanol concentrations tend to produce larger, highly crystalline nanoparticles (Ghorbani *et al.* 2020; Allegretto *et al.* 2024).

SEM elemental mapping (Figure 15) demonstrated uniform distribution of Zn throughout the film, indicating strong interactions between Zn^{2+} ions and the gluten matrix, consistent with the observed improvements in tensile strength and reduced water vapor transmission. EDS analysis (Figure 16, Table 3) confirmed the presence of C, N, and O from gluten, glycerol, and imidazole, with Zn originating from ZIF-8, and no contaminants were detected, indicating high film purity.

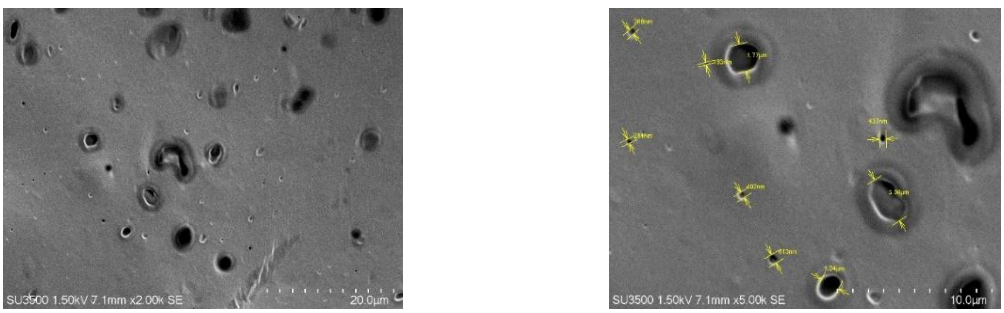

(a) (b)

Figure 14. SEM micrographs showing the surface microstructure of Glu/Gly/0.75% ZIF-8 EF at (a) 2000× and (b) 5000× magnifications, highlighting the smooth polymer matrix and well-dispersed ZIF-8 particles

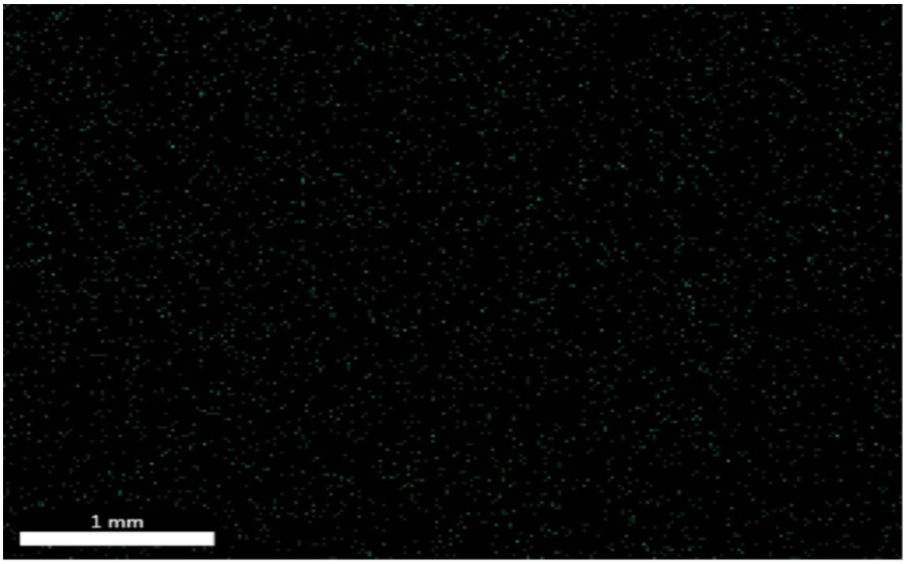

Figure 15. Elemental mapping of Zn in Glu/Gly/0.75% ZIF-8 EF, illustrating the uniform distribution of zinc throughout the edible film matrix

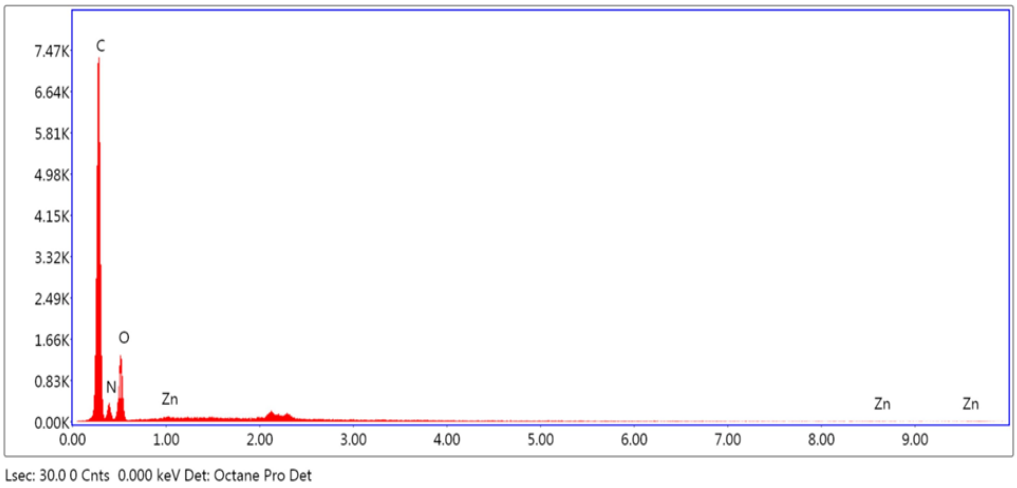

Figure 16. EDS spectrum of Glu/Gly/0.75% ZIF-8 EF, showing the elemental composition

Table 3. Elemental composition of Glu/Gly/0.75% ZIF-8 EF as determined by EDS analysis, showing the relative percentages of C, N, O, and Zn, confirming the incorporation of ZIF-8 without detectable contaminants

Element	Weight %	Atomic %
C K	56.46	62.08
N K	18.66	17.60
O K	24.53	20.25
ZnK	0.35	0.07

These results align with previous reports on ZIF-8-incorporated biocomposites, where SEM-EDS analysis confirmed uniform dispersion of hexagonal ZIF-8, enhancing mechanical performance and antimicrobial properties (Makhetha *et al.* 2020). Incorporation of ZIF-8 nanoparticles increased surface roughness, which correlated with higher water contact angles and improved nanoparticle distribution. Additionally, the intrinsic porosity of ZIF-8 reduced water vapor permeability by blocking potential gas channels between polymer macromolecules, consistent with observations in PVA/starch/methyl cellulose composites (Lee *et al.* 2019). Overall, these findings demonstrate that ZIF-8 incorporation significantly enhances the structural, barrier, and functional properties of Glu/Gly-based edible films, highlighting their potential for high-performance food packaging applications.

CONCLUSION

The incorporation of ZIF-8 into Glu/Gly edible films (GBEF) significantly enhanced their functional, physicochemical, and biological properties, confirming the potential of Glu/Gly/ZIF-8 EF as an active food packaging material. The addition of ZIF-8 improved water vapor barrier and hydrophobicity, leading to a marked decrease in WVTR without significantly affecting film thickness. Mechanical testing revealed that tensile strength (TS) increased up to 60.583 MPa for Glu/Gly/0.75% ZIF-8 EF, while elongation at break (EAB) reached 382.83% for Glu/Gly/0.25% ZIF-8 EF, representing 1.5- to 8.5-fold improvements compared to films containing ZnO nanoparticles. FTIR analysis confirmed the presence of ZIF-8 through characteristic shifts in N–H, C–H, and α-helix absorption bands, as well as the detection of imidazole and Zn–N groups, indicating physical incorporation rather than chemical reaction with the Glu/Gly matrix. SEM imaging demonstrated a relatively smooth and homogeneously distributed ZIF-8 surface with particle sizes ranging from 63 nm to 3.04 μm, while EDS analysis confirmed the elemental composition with no detectable contaminants. Biologically, Glu/Gly/ZIF-8 EF exhibited strong antibacterial activity, with inhibition zones of 25–26 mm for *E. coli* and 25–34 mm for *S. aureus*, highlighting its potential for controlling both Gram-negative and Gram-positive pathogens. Taken together, these results demonstrate that ZIF-8 effectively enhances the structural, rheological, and antimicrobial performance of gluten-based films, addressing the study's objectives of evaluating reproducibility, integrity, and functional properties. Future research should explore optimization of ZIF-8 particle size and distribution, long-term stability under storage conditions, and the application of Glu/Gly/ZIF-8 EF to real food systems to fully realize its potential as an active and sustainable packaging material.

ACKNOWLEDGMENT

The authors gratefully acknowledge the data support provided by Politeknik Negeri Bandung and the laboratory facilities made available by Institut Teknologi Bandung. This work was supported by the Center for Research and Community Services, Politeknik Negeri Bandung, under Contract No. B/3.29/PL1.R7/PG.00.03/2024.

REFERENCES

Abdullah-Al-Rahim, M. (2021). A Review of wheat gluten-based bioplastics processing and their applications. Ph.D thesis. Faculty of Agriculture and Applied Science. North Dakota State University.

Ahmad, N., Nordin, N.A., Jaafar, J., Malek, N.A., Ismail, A.F., Yahya, M.N., Hanim, S.A.M. & Abdullah, M.S. (2020). Eco-friendly method for synthesis of zeolitic imidazolate framework 8 decorated graphene oxide for antibacterial activity enhancement. *Particuology*. **49**: 24-32.

Allegretto, J.A., Onna, D., Bilmes, S.A., Azzaroni, O. & Rafti, M. (2024). Unified roadmap for ZIF-8 nucleation and growth: Machine learning analysis of synthetic variables and their impact on particle size and morphology. *Chemistry of Materials*. **36(11)**: 5814–5825.

Azam, S.U., Hussain, A., Farrukh, S., Noor, T. & Liu, Y. (2020). Enhancement in the selectivity of O2/N2 via ZIF-8/CA mixed-matrix membranes and the development of a thermodynamic model to predict the permeability of gases. *Environmental Science and Pollution Research*. **27(19)**: 24413–24429.

Azari, S.S., Alizadeh, A., Roufegarinejad, L., Asefi, N. & Hamishehkar, H. (2021). Preparation and characterization of gelatin/β-glucan nanocomposite film incorporated with ZnO nanoparticles as an active food packaging system. *Journal of Polymers and the Environment*. **29(12)**: 1143–1152.

Barazi, A.Ö., Mehmetoğlu, A.Ç. & Erkmen, O. (2023). A novel edible coating produced from wheat gluten, *Pistacia vera* L. resin, and essential oil blend: Antimicrobial effects and sensory properties on chicken breast fillets. *Foods*. **12(12)**: 1-17.

Bora, D., Duarah, R., Barman, P., Jarugala, J. & Sadiku, E.R. (2024). Development of Eco-friendly and durable composites: polypropylene carbonate (PPC)–Polylactic acid (PLA)/ZIF-8 for packaging applications. *ACS Applied Polymer Materials*. **6(17)**: 10380–10392.

Caamaño, K., López-Carballo, G., Heras-Mozos, R., Glatz, J., Hernández-Muñoz, P., Gavara, R., & Giménez-Marqués, M. (2023). ZIF-8 encapsulation improves the antifungal activity of benzaldehyde and methyl anthranilate in films. *Dalton Transactions*. **52(47)**: 17993-17999.

Cazón, P., Morales-Sanchez, E., Velazquez, G. & Vázquez, M. (2022). Measurement of the water vapor permeability of chitosan films: A laboratory experiment on food packaging materials. *Journal of Chemical Education*. **99(6)**: 2403–2408.

Channab, B.E., Idrissi, A.E., Ammar, A., Akil, A., White, J.C. & Zahouily, M. (2024). ZIF-8 metal-organic framework, carboxymethylcellulose and polyvinyl alcohol bio-nanocomposite controlled-release phosphorus fertilizer: Improved P management and tomato growth. *Chemical Engineering Journal*. **495**: 1-16.

Chen, P., Xie, F., Tang, F. & McNally, T. (2021). Influence of plasticiser type and nanoclay on the properties of chitosan-based materials. *European Polymer Journal*. **144**: 1-10.

Dirpan, A., Ainani, A.F. & Djalal, M. (2023). A review on biopolymer-based biodegradable film for food packaging: trends over the last decade and future research. Polymers. **15(13)**: 1-33.

Djenar, N.S., Jayanti, R.D. & Suryadi, J. (2021). The effect of sodium chloride with varying concentration on characteristics and rheology of extracted gluten from wheat flour. *In Proceedings of the 2nd International Seminar of Science and Applied Technology (ISSAT 2021)*. Atlantis Press. Bandung, 23 November 2021. pp. 20-25.

Djenar, N. S., Jayanti, R. D., Wilson, W. & Qinthara, Z. M. (2024a). The Effect of sodium sulfite with varying concentration on the separation of gliadin from gluten. *In 4th International Seminar on Fundamental and Application of Chemical Engineering (ISFAChE)*. Trans Tech Publications Ltd. Surabaya, 26-27 Oktober 2022. pp. 3-12

Djenar, N.S., Fulazzaky, M.A., Rinaldi, K., Santoso, B., Sulaeman, S.A., Mardiah, M., Fan, H. & Yulianthina, S. (2024b). Evaluation of a gluten-based edible film incorporated with beetroot extract and ZnO nanoparticles as an active food packaging system. *ACS Food Science & Technology*. **4(6)**: 1511–1526.

García-Palacín, M., Martínez, J.I., Paseta, L., Deacon, A., Johnson, T., Malankowska, M., Téllez, C. & Coronas, J. (2020). Size-controlled ZIF-8 nanoparticle synthesis from recycled mother liquors: Environmental impact assessment. *ACS Sustainable Chemistry & Engineering*. **8(7)**: 2973–2980.

Geng, C., Liu, X., Ma, J., Ban, H., Bian, H. & Huang, G. (2023). High strength, controlled release of curcumin-loaded ZIF-8/chitosan/zein film with excellence gas barrier and antibacterial activity for litchi preservation. *Carbohydrate Polymers*. 306: 1-13.

Ghorbani, H., Ghahramaninezhad, M. & Shahrak, M. N. (2020). The effect of organic and ionic liquid solvents on structure crystallinity and crystallite size of ZIF-8 for CO_2 uptake. *Journal of Solid State Chemistry*. 289: 1-8.

Hara, Y., Castell-Perez, M.E. & Moreira, R.G. (2023). Properties of poly (vinyl alcohol) films with embedded zeolitic imidazolate framework (ZIF-8) nanoparticles for food packaging applications. *Journal of Food Science*. **88(5)**: 2078–2089.

Hu, J., Pan, Y.T., Zhou, K., Song, P. & Yang, R. (2024). A new way to improve the fire safety of polyurethane composites with the assistance of metal–organic frameworks. *RSC Applied Polymers*. **2(6)**: 996-1012.

Jiang, L., Ye, R., Xie, C., Wang, F., Zhang, R., Tang, H., He, Z., Han, J. & Liu, Y. (2023). Development of zein edible films containing different catechin/cyclodextrin metal-organic frameworks: Physicochemical characterization, antioxidant stability and release behavior. LWT. **173**: 1-9.

Karnwal, A., Rauf, A., Jassim, A.Y., Selvaraj, M., Al-Tawaha, A.R.M.S., Kashyap, P., Kumar, D. & Malik, T. (2025). Advanced starch-based films for food packaging: Innovations in sustainability and functional properties. *Food Chemistry: X*. **29**: 1-21.

Kermanshahi, P.K. & Akhbari, K. (2024). The antibacterial activity of three zeolitic-imidazolate frameworks and zinc oxide nanoparticles derived from them. *RSC Advances*. **14(8)**: 5601–5608.

Khashayary, S. & Aarabi, A. (2021). Evaluation of physico-mechanical and antifungal properties of gluten-based film incorporated with vanillin, salicylic acid, and montmorillonite (Cloisite 15A). *Food and Bioprocess Technology*. **14(1)**: 665–678.

Kłosok, K., Welc, R., Fornal, E. & Nawrocka, A. (2021). Effects of physical and chemical factors on the structure of gluten, gliadins and glutenins as studied with spectroscopic methods. *Molecules*. **26(2)**: 1-21.

Krekora, M. & Nawrocka, A. (2022). The influence of selected polyphenols on the gluten structure - A study on gluten dough with application of FT-IR and FT-Raman spectroscopy. *Journal of Cereal Science*. **108**: 1-8.

Kumar, V.A., Hasan, M., Mangaraj, S., Pravitha, M., Verma, D.K. & Srivastav, P.P. (2022). Trends in edible packaging films and prospective future in food. *Applied Food Research*. **2(1)**: 1-17.

Lee, S., Lei, Y., Wang, D., Li, C., Cheng, J., Wang, J., Meng, W. & Liu, M. (2019). The study of zeolitic imidazolate framework (ZIF-8) doped polyvinyl alcohol/starch/methyl cellulose blend film. *Polymers*. **11(12)**: 1-16.

Li, X., Tu, Z.C., Sha, X.M., Ye, Y.H., & Li, Z.Y. (2020). Flavor, antimicrobial activity, and physical properties of composite film prepared with different surfactants. *Food Science & Nutrition*. **8(7)**: 3099-3109.

Li, Y., Shan, P., Yu, F., Li, H. & Peng, L. (2023). Fabrication and characterization of waste fish scale-derived gelatin/sodium alginate/carvacrol loaded ZIF-8 nanoparticles composite films with sustained antibacterial activity for active food packaging. *International Journal of Biological Macromolecules*. **230**: 1-16.

Liu, Y., Zhang, J.,& Tan, X. (2019). High Performance of PIM-1/ZIF-8 composite membranes for O_2/N_2 separation. *ACS Omega*. **4(15)**: 16572–16577.

Makhetha, T.A., Ray, S.C. & Moutloali, R.M. (2020). Zeolitic imidazolate framework-8-encapsulated nanoparticle of Ag/Cu Composites supported on graphene oxide: synthesis and

antibacterial activity. *ACS Omega*. **5(17)**: 9626–9640.

Masibi, E.G., Makhetha, T.A. & Moutloali, R. M. (2022). Effect of the Incorporation of ZIF-8@GO into the Thin-Film Membrane on Salt Rejection and BSA Fouling. *Membranes*. **12(4)**: 1-23.

Motelica, L., Ficai, D., Oprea, O., Ficai, A., Trusca, R.-D., Andronescu, E., & Holban, A. M. (2021). Biodegradable alginate films with zno nanoparticles and citronella essential oil—a novel antimicrobial structure. *Pharmaceutics*. **13(7)**: 1-24.

Pires, A.F., Díaz, O., Cobos, A. & Pereira, C. D. (2024). A review of recent developments in edible films and coatings – focus on whey-based materials. *Foods*. **13(16)**: 1-24.

Sani, M.A., Khezerlou, A. & McClements, D. J. (2024). Zeolitic imidazolate frameworks (ZIFs): advanced nanostructured materials to enhance the functional performance of food packaging materials. *Advances in Colloid and Interface Science.* **327**: 1-21.

Sharanyakanth, P.S. & Radhakrishnan, M. (2020). Synthesis of metal-organic frameworks (MOFs) and its application in food packaging: A review. *Trends in Food Science & Technology*. **104**: 102–116.

Shen, M., Forghani, F., Kong, X., Liu, D., Ye, X., Chen, S. & Ding, T. (2020). Antibacterial applications of metal–organic frameworks and their composites. *Comprehensive Reviews in Food Science and Food Safety*. **19(4)**: 1397-1419.

Shen, B., Wang, Y., Wang, X., Amal, F.E., Zhu, L. & Jiang, L. (2022). A cruciform petal-like (ZIF-8) with bactericidal activity against foodborne gram-positive bacteria for antibacterial food packaging. *International Journal of Molecular Sciences.* **23(14)**: 1-16.

Tezerjani, A.A., Halladj, R. & Askari, S. (2021). Different view of solvent effect on the synthesis methods of zeolitic imidazolate framework-8 to tuning the crystal structure and properties. *RSC Advances*. **11(32)**: 19914-19923.

Vida, G., Szunics, L., Veisz, O. & Cséplő, M. (2022). Breeding for improved gluten strength and yellow pigment content in winter durum wheat. *Bulgarian Journal of Crop Science*. **59(6)**: 16-33.

Wan, N.H., Nafchi, A.M. & Huda, N. (2018). Tensile strength, elongation at breaking point and surface color of a biodegradable film based on a duck feet gelatin and polyvinyl alcohol blend. *Asia Pacific Journal of Sustainable Agriculture, Food and Energy*. **6(2)**: 16-21.

Wang, L., Cheng, S., Qin, K., Yang, X., Wang, H., Man, C., Zhao, Q. & Jiang, Y. (2023a). Apigenin@ZIF-8 with pH-responsive sustained release function added to propolis-gelatin films achieved an outstanding antibacterial effect. *Food Packaging and Shelf Life*. **40(8)**: 1-9.

Wang, M., Nian, L., Wu, J., Cheng, S., Yang, Z. & Cao, C. (2023b). Visible light-responsive chitosan/sodium alginate/QDs@ZIF-8 nanocomposite films with antibacterial and ethylene scavenging performance for kiwifruit preservation. *Food Hydrocolloids*. **145(28)**: 1-13.

Wang, J., Sun, X., Xu, X., Sun, Q., Li, M., Wang, Y. & Xie, F. (2022). Wheat-flour-based edible films: Effect of gluten on the rheological properties, structure, and film characteristics. *International Journal of Molecular Sciences*. **23(19)**: 1-17.

Wu, Y., Gao, S., Zhao, J., Kong, S., Wang, H. & Hou, H. (2024). Sugar/sugar alcohol with glycerol as co-plasticizers for high-content starch/PBAT blown films: from fine structure to physicochemical properties. *Journal of the Science of Food and Agriculture*. **105(2)**: 1105–1115.

Xing, Y., Li, W., Wang, Q., Li, X., Xu, Q., Guo, X., Bi, X., Liu, X., Shui, Y., Lin, H. & Yang, H. (2019). Antimicrobial nanoparticles incorporated in edible coatings and films for the preservation of fruits and vegetables. *Molecules*. **24(9)**: 1-30.

Xu, J. & Li, Y. (2023). Wheat gluten-based coatings and films: Preparation, properties, and applications. *Journal of Food Science*. **88(2)**: 582–594.

Zhang, Y., Deng, L., Zhong, H., Pan, J., Li, Y. & Zhang, H. (2020). Superior water stability and antimicrobial activity of electrospun gluten nanofibrous films incorporated with glycerol monolaurate. *Food Hydrocolloids*. **109**: 1-8.

Zhao, J., Wei, F., Xu, W. & Han, X. (2020). Enhanced antibacterial performance of gelatin/chitosan film containing capsaicin loaded MOFs for food packaging. *Applied Surface Science*. **510**: 1-9.

Zhou, X., Yang, R., Wang, B. & Chen, K. (2019). Development and characterization of bilayer films based on pea starch/polylactic acid and use in the cherry tomatoes packaging. *Carbohydrate Polymers*. **222**: 1-7.

Zhu, C., Chang, D., Wang, X., Chai, D., Chen, L., Dong, A. & Gao, G. (2019). Novel antibacterial fibers of amphiphilic N-halamine polymer prepared by electrospinning. *Polymers for Advanced Technologies*. **30(6)**: 1386-1393.